

Preparation and evaluation of superparamagnetic surface molecularly imprinted polymer nanoparticles for selective extraction of bisphenol A in packed food

Zhou Xu,^{ab} Li Ding,^b Yanjiao Long,^c LiGuang Xu,^a Libing Wang^{*ab} and Chuailai Xu^{*a}

Received 9th April 2011, Accepted 18th May 2011

DOI: 10.1039/c1ay05206c

Molecularly imprinted polymer (MIP) coated Fe_3O_4 nanoparticles ($\text{Fe}_3\text{O}_4@\text{MIP}$) were synthesized by atom transfer radical polymerization (ATRP) and used as highly selective magnetic solid-phase extraction (MSPE) sorbents for trace bisphenol A (BPA) from packed food. The morphological and polymeric characteristics of the $\text{Fe}_3\text{O}_4@\text{MIP}$ were characterized by transmission electron microscopy and Fourier transform infrared spectroscopy. In this work, competitive recognition compounds (4-*n*-octylphenol and bisphenol A diglycidyl ether) exhibited lower binding capability to the $\text{Fe}_3\text{O}_4@\text{MIP}$ than BPA. A high performance liquid chromatography with fluorescence detection (HPLC-FLD) method was developed for the determination of BPA in canned orange and milk samples. The main factors influencing the extraction efficiency, including high specificity, the amount of surfactant, the shaking time and the desorption ability of complex food matrices were investigated and optimized. Various parameters such as the pH of the sample, the amount of $\text{Fe}_3\text{O}_4@\text{MIP}$ sorbent, the extraction time, and the desorption conditions were optimized. Notably, the extraction can be carried out quickly, and the extraction time for BPA onto $\text{Fe}_3\text{O}_4@\text{MIP}$ sorbents can be clearly shortened to 5 min. Good linearities ($r^2 > 0.9965$) for all calibration curves were obtained, and the limit of detection (LOD) for BPA was 0.1 and 0.3 ng mL⁻¹ in canned orange and milk samples, respectively. To the best of our knowledge, this is the first time that surface molecularly imprinted polymer nanoparticles have been used for the pretreatment of packed food.

Introduction

During the last decade, there has been a worldwide scientific and public discussion about the potential consequences of long-term dietary exposure to endocrine disrupters. Among these substances, bisphenol A (BPA) is mainly used as a monomer in the production of epoxide resins and polycarbonate plastics, and as an antioxidant or stabilizer in PVC plastics, while the major types of interior can coating are made from epoxy resins. Food packaging mainly consists of metal cans and PVC plastic. The migration of BPA from interior can coating and PVC products into food could affect human health.^{1,2} Several analytical methods have been reported for the quantification of BPA in packed food, such as HPLC/UV,³ LC/MS⁴ and GC/MS.⁵

Generally, for chromatographic analysis of small molecular compounds in packed food such as milk and canned food,

sample pretreatment is required to clean up the sample before injection. A literature survey reveals that there have been a number of pretreatment methods for analysis of BPA in packed food components, such as liquid–liquid phase extraction (LLE)⁶ and solid-phase dispersion (SPE).⁷ However, these methods still have some limitations or shortcomings, such as the need for sample dilution and incomplete protein precipitation. Compared with traditional LLE and SPE, magnetic solid-phase extraction (MSPE) has many obvious advantages including low consumption of organic solvents, high breakthrough volume, easy elution of analytes and a simple cleanup step. Moreover, MSPE need not be packed into the SPE cartridge. However, in most cases, novel MSPE methods can not recognize and specially bind the target molecule. Novel MSPE methods have been developed based on magnetic nanoparticles modified by hemimicelles^{8–13} or mesoporous SiO_2 ,¹⁴ carbon,¹⁵ ZrO_2 ,¹⁶ TiO_2 ¹⁷ and Al_2O_3 ,^{18,19} which can adsorb target compounds through electrostatic attraction, ion-exchange, hydrophobic/hydrophilic and polar/nonpolar interactions. Novel magnetic nanoparticle MSPE sorbents with high specificities, simple preparation processes, high adsorption efficiencies and low cost should be developed for food analysis.

Molecular imprinted polymers (MIP) are a promising and facile separation material to produce molecule-specific

^aSchool of Food Science and Technology, State Key Lab of Food Science and Technology, Jiangnan University, Wuxi, 214122, P R China. E-mail: wanglb0419@126.com; Fax: +86-73185627820; Tel: +86-73185627812

^bHunan Entry–Exit Inspection and Quarantine Bureau of the People's Republic of China, Changsha, 410004, P R China

^cGuangdong Entry–Exit Inspection and Quarantine Bureau of the People's Republic of China, Guangzhou, 510623, P R China

recognition sites in synthetic polymers that selectively bind template molecules.^{20–22} If a thin layer of MIP is covered onto the surface of magnetic nanoparticles to form MIP coated Fe_3O_4 nanoparticles ($\text{Fe}_3\text{O}_4@\text{MIP}$) SPE sorbents, the specific combination problem should be overcome. Moreover, the nanoscale $\text{Fe}_3\text{O}_4@\text{MIP}$ SPE sorbents combine strong recognition ability of materials, superparamagnetism of magnetic materials, and high surface area of nanomaterials. However, traditional MIP tended to have sharp-edged, irregular MIP areas and recognition sites within the polymer bulk, and did not form uniform MIP shells for practical MSPE application.²³ The new report by Qin²⁴ *et al.* avoided solution polymerization and resulting gelation compared with traditional MIP. Atom transfer radical polymerization (ATRP) has been proposed as a new surface imprinting technology,^{25–27} which is a new class of controlled living radical polymerization.²⁸ Compared with the present MIP, the thickness of MIP on Fe_3O_4 nanoparticles can be well controlled by the ATRP reagent.

Gai *et al.* have grafted magnetic particles with MIP by ATRP for highly selective adsorption and recognition of protein.²⁹ Lu *et al.* have synthesized MIP coated nanoparticles *via* surface imprinting technology, which can be directly used in separating sorbent assays.^{30–32} However, these previously reported methods are simply applied to detection in water. To the best of our knowledge, there is no report about the application of $\text{Fe}_3\text{O}_4@\text{MIP}$ nanoparticles prepared by ATRP as MSPE sorbents for food analysis.

Herein, we report the preparation and characterization of $\text{Fe}_3\text{O}_4@\text{MIP}$ nanoparticles and their potential application in canned orange and milk samples. Extraction conditions including the pH of the solution, amount of nanoparticle sorbent, equilibrium time, and desorption conditions were optimized. By coupling this MSPE technique with HPLC with fluorescence detection (FLD), a highly selective and sensitive MSPE-HPLC-FLD analytical method was established.

Experimental

Materials and reagents

The standards of bisphenol A (BPA), 4-*n*-octylphenol (4-*n*-OP) and bisphenol A diglycidyl ether (BADGE) were purchased from Dr Ehrenstorfer (Augsburg, Germany). HPLC-grade methanol (E. Merck, Darmstadt, Germany) was used for HPLC analysis. 3-Amino-propyltrimethoxysilane, 1,1',4,7,7'-pentamethyldiethylenetriamine (PMDETA), 4-VP, ethylene and glycol dimethacrylate (EGDMA), tetraethyl orthosilicate (TEOS) were obtained from J&K Chemical (Tianjin, China). 2-Bromoisobutyryl bromide and ferric chloride ($\text{FeCl}_3 \cdot 6\text{H}_2\text{O}$) were supplied by Acros (New Jersey, USA). 2-Bromoisobutyryl bromide and CuBr were obtained from Sigma-Aldrich (St. Louis, MO, USA). All the other reagents were of analytical grade, including acetonitrile, triethylamine, zinc acetate, potassium ferrocyanide and acetone. Milli-Q ultrapure water (18.2 M Ω) was used in all experiments.

Apparatus

The $\text{Fe}_3\text{O}_4@\text{MIP}$ composite was characterized using a JEOL JEM-3010 transmission electron microscope (Jeol, Japan).

FT-IR spectra were obtained with a Thermo Nicolet 670 FT-IR instrument (Thermo, USA). Chromatographic analysis was carried out on an Agilent 1200 LC system (Agilent, Germany) equipped with automatic injector and fluorescence detection (FLD).

Preparation of $\text{Fe}_3\text{O}_4@\text{MIP}$ composite

The magnetic nanoparticles (Fe_3O_4) were prepared through a solvothermal reaction. 2 g of $\text{FeCl}_3 \cdot 6\text{H}_2\text{O}$ was dissolved in ethylene glycol (60 mL) to form a clear solution, followed by the addition of NaAc (4.8 g) and polyethylene glycol 4000 (1.5 g). The mixture was stirred vigorously for 2 h and then sealed in a Teflon-lined stainless-steel autoclave (100 mL capacity). The autoclave was heated at 210 °C for 12 h, and then allowed to cool to room temperature. The black products were washed several times with ethanol and dried in vacuum at room temperature for 6 h.

0.30 g of Fe_3O_4 particles (~150 nm in diameter) were treated with 0.1 M HCl aqueous solution (100 mL) by ultrasonication. After 10 min, the magnetite nanoparticles were separated and washed with deionized water, and then homogeneously dispersed in a mixture of ethanol (120 mL), ultrapure water (30 mL) and concentrated ammonia aqueous solution (1.5 mL, 28 wt.%), followed by the addition of tetraethyl orthosilicate (TEOS, 3 mL). After stirring at 20 °C for 16 h, the $\text{Fe}_3\text{O}_4@\text{SiO}_2$ nanoparticles were washed with ethanol and water and dried under vacuum at room temperature for 6 h.

Dried $\text{Fe}_3\text{O}_4@\text{SiO}_2$ (200 mg), 3-amino-propyltrimethoxysilane (1 mL) and absolutely dry toluene (40 mL) were mixed in a boiling 3-neck flask under nitrogen atmosphere. With mechanical stirring, the mixture was allowed to react at a constant temperature of 90 °C for 48 h, and the nanoparticles produced were separated from the mixture by a magnet (Nd-Fe-B, 60 × 60 × 30 mm). The product was washed 5 times with toluene then 5 times with methanol. Amino-modified $\text{Fe}_3\text{O}_4@\text{SiO}_2$ (200 mg), toluene (20 mL), triethylamine (500 μ L), and a catalytic amount of DMAP (500 mg) were added individually into a conical flask. Then 2-bromoisobutyryl bromide (400 μ L) was added, and the mixture was kept first at 0 °C for 2 h and then at room temperature for 24 h. The product was separated from the mixture by a magnet. For purification, the $\text{Fe}_3\text{O}_4@\text{SiO}_2@\text{Br}$ was washed 5 times with dichloromethane.

The preparation of $\text{Fe}_3\text{O}_4@\text{MIP}$ nanoparticles was performed in a conical flask containing 50 mg of $\text{Fe}_3\text{O}_4@\text{SiO}_2@\text{Br}$ suspended in a polymerization mixture consisting of CuBr (14.4 mg), 1,1',4,7,7' -pentamethyldiethylenetriamine (6.25 mL), the functional monomer 4-VP (630 μ L), the cross-linking monomer EGDMA (30 mmol), and template bisphenol A (228 mg) dissolved in 15 mL acetonitrile. After sealing, mixing, and purging the mixture with nitrogen, the flask was placed in a temperature-controlled oil bath at 70 °C with mechanical stirring for 24 h. The reaction product was then separated from the polymerization mixture by a magnet. The control $\text{Fe}_3\text{O}_4@\text{NIP}$ nanoparticles were prepared and washed using the same procedures as above but without the addition of the template bisphenol A.

SPE procedure

$\text{Fe}_3\text{O}_4@\text{MIP}$ extraction of all samples involved in this study was carried out in 50 mL centrifuge tubes. A sample volume of 20 mL was adopted throughout the study. The canned orange sample was diluted to 30 mL with phosphate buffer at pH 8.9. The milk sample, diluted to 30 mL with phosphate buffer at pH 8.9, was added to 500 μL zinc acetate (1 M) and potassium ferrocyanide (0.2 M), respectively, to remove the protein.

After being shaken for 1 min and centrifuged at 7500 r min^{-1} for 3 min, the supernatant was collected, and the precipitated protein was rinsed twice with 2 mL methanol. Then the supernatant, the eluate and 15 mg of $\text{Fe}_3\text{O}_4@\text{MIP}$ were mixed and diluted to 50 mL, with the pH adjusted to ~ 8.9 . The mixture was shaken for 3 min. After standing for 10 min, $\text{Fe}_3\text{O}_4@\text{MIP}$ was separated rapidly from the solution with an external magnet. After discarding the supernatant solution, the analytes were eluted from the isolated particles four times with 2 mL methanol (containing 0.6% acetic acid, v/v). The methanol desorption solvent was then filtered through a 0.22 μm membrane filter and was ready for LC-FLD analysis. The $\text{Fe}_3\text{O}_4@\text{MIP}$ preparation and extraction process was illustrated in Scheme 1.

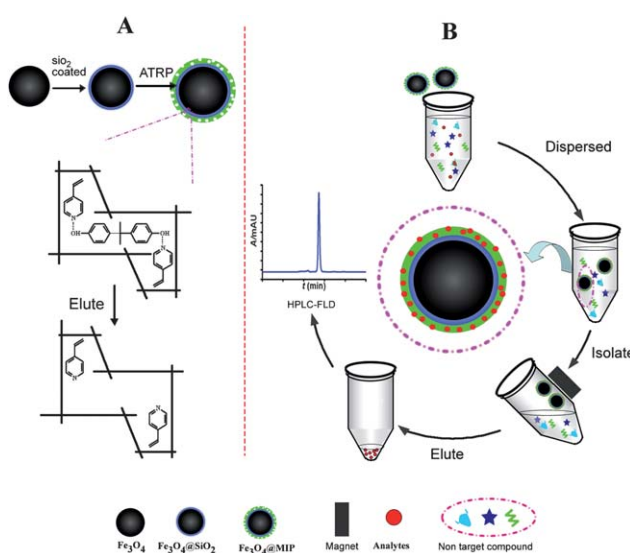
LC-FLD analysis

A Waters C18 column (250 mm \times 4.6 mm ID, 3.5 μm) was used for LC separation. The mobile phase was composed of A (water)–B (methanol) with a gradient elution (0–10 min, isocratic conditions with 30% of methanol). Other analysis conditions were as follows: column temperature, 25 °C; flow rate, 1.0 mL min^{-1} ; injection volume, 10 μL . The detection wavelengths were selected as 275 and 305 nm for excitation and emission, respectively. Samples were filtered through a 0.22 μm membrane prior to injection.

Results and discussion

Characterization of $\text{Fe}_3\text{O}_4@\text{MIP}$

Previous research has shown that dense polymer shells with tunable thickness can be easily grafted from the surfaces of solids



Scheme 1 The preparation of $\text{Fe}_3\text{O}_4@\text{MIP}$ and its application for enriching the active compounds as an MSPE sorbent.

or nanoparticles with controlled behavior *via* surface initiated ATRP. The resulting superparamagnetic surface-imprinted nanoparticles (designated $\text{Fe}_3\text{O}_4@\text{MIP}$) were characterized by transmission electron microscopy (TEM). From the TEM images (Fig. 1B and C), a polymer shell with well defined shape and configuration was readily observed on the surface of $\text{Fe}_3\text{O}_4@\text{SiO}_2$ nanoparticles with light contrast. The polymer shell had an average thickness of about 20–40 nm and appeared to be uniform.

It is important that the adsorbents should possess superparamagnetic properties to realize rapid separation in a magnetic field. Fig. 2 shows the magnetization curves of Fe_3O_4 , $\text{Fe}_3\text{O}_4@\text{SiO}_2$ and $\text{Fe}_3\text{O}_4@\text{MIP}$ at room temperature. All Fe_3O_4 , $\text{Fe}_3\text{O}_4@\text{SiO}_2$ and $\text{Fe}_3\text{O}_4@\text{MIP}$ exhibit typical superparamagnetic behavior with no hysteresis, remanence and coercivity. The maximal saturation magnetizations of Fe_3O_4 , $\text{Fe}_3\text{O}_4@\text{SiO}_2$ and $\text{Fe}_3\text{O}_4@\text{MIP}$ are 69.45, 55.49 and 35.78 emu g^{-1} , respectively. The decrease in maximal saturation magnetization of $\text{Fe}_3\text{O}_4@\text{MIP}$ results from the nonmagnetic SiO_2 and MIP shell. Ji *et al.* have reported that magnetic molecularly imprinted polymers were prepared by miniemulsion polymerization with a saturation magnetization of 18 emu g^{-1} .²³ The saturation magnetization of the $\text{Fe}_3\text{O}_4@\text{MIP}$ prepared here is higher in comparison due to the smaller particle size of $\text{Fe}_3\text{O}_4@\text{MIP}$. Once the external magnetic field is taken away, these sorbents can redisperse rapidly.

FT-IR spectra of Fe_3O_4 , $\text{Fe}_3\text{O}_4@\text{SiO}_2$, and $\text{Fe}_3\text{O}_4@\text{MIP}$ were obtained to verify that the expected products were obtained (see Fig. 3). The characteristic band of Fe–O appeared at about 582 cm^{-1} in each spectrum. The Si–OH vibration peak at 952 cm^{-1} and the Si–O–Si vibration peak at around 1094 cm^{-1} were also observed, indicating that the SiO_2 shell was indeed coated onto the surfaces of Fe_3O_4 nanoparticles. An intense peak at 1405 cm^{-1} proved that C–N from pyridyl existed in the polymer. Upon comparing $\text{Fe}_3\text{O}_4@\text{MIP}$ to $\text{Fe}_3\text{O}_4@\text{SiO}_2$, the intensity of the C–H adsorption band at 2926 cm^{-1} is clearly greater for $\text{Fe}_3\text{O}_4@\text{MIP}$; moreover, Si–OH of the silica shell vanished for $\text{Fe}_3\text{O}_4@\text{MIP}$. Such results confirmed that the polymerization was successful.

Evaluation of adsorption capacity and specificity of $\text{Fe}_3\text{O}_4@\text{MIP}$

The adsorption capacity and selectivity are important factors in the evaluation of the MIPs. BPA, BDAGE, and 4-OP solutions within the concentration range of 0.05–0.5 mg mL^{-1} were studied. As shown in Fig. 4, the amount of adsorbed BPA increased with increasing initial concentration of BPA solution. The static adsorption capacity of the $\text{Fe}_3\text{O}_4@\text{MIP}$ sorbent for BPA was calculated as 0.3 mg mL^{-1} . The static adsorption capacity of the $\text{Fe}_3\text{O}_4@\text{MIP}$ sorbent was about three times that of the $\text{Fe}_3\text{O}_4@\text{NIP}$ sorbent. To further evaluate the specificity of the $\text{Fe}_3\text{O}_4@\text{MIP}$ nanoparticles, the binding of several structurally related compounds to $\text{Fe}_3\text{O}_4@\text{MIP}$ nanoparticles was studied and compared. All the evaluated compounds exhibited lower binding capability to $\text{Fe}_3\text{O}_4@\text{MIP}$ nanoparticles than the original template. In general, the $\text{Fe}_3\text{O}_4@\text{MIP}$ possesses both specific and nonspecific binding sites, while the $\text{Fe}_3\text{O}_4@\text{NIP}$ only has nonspecific binding sites, which enables the $\text{Fe}_3\text{O}_4@\text{MIP}$ to

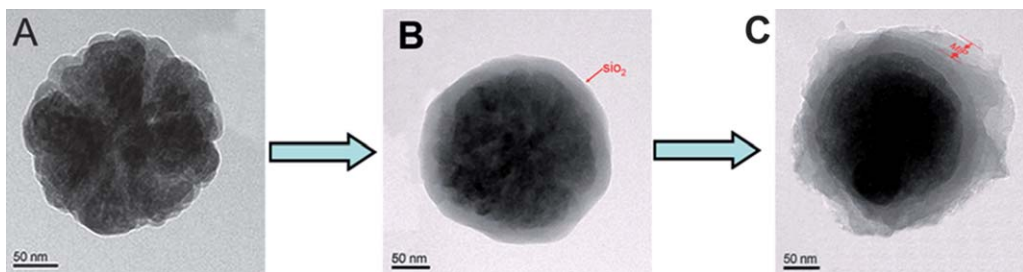


Fig. 1 TEM images of magnetic Fe₃O₄ nanoparticles (A), Fe₃O₄@SiO₂ (B) and Fe₃O₄@MIP composites (C).

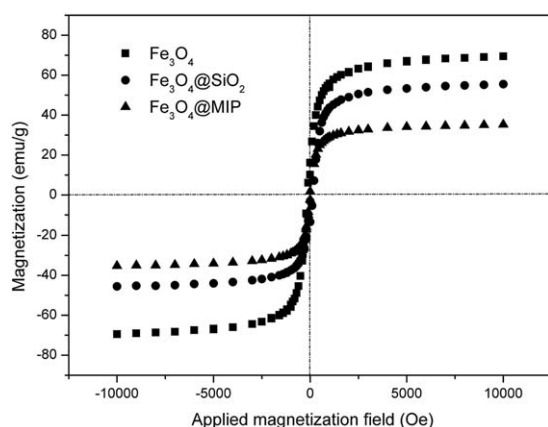


Fig. 2 VSM magnetization curves for Fe₃O₄, Fe₃O₄@SiO₂ and Fe₃O₄@MIP.

take up more BPA than the Fe₃O₄@NIP. The results showed that the Fe₃O₄@MIP sorbent had a higher adsorption capacity for BPA than other ordinary sorbents. So, the Fe₃O₄@MIP sorbent would be better for the enrichment of trace BPA in samples.

In order to verify that the Fe₃O₄@MIP was selective for BPA, two different analogues (BADGE and 4-OP) were selected to test the binding characteristics of the Fe₃O₄@MIP and the Fe₃O₄@NIP. As shown in Table 1, the specificity of Fe₃O₄@MIP was estimated by measuring the distribution coefficients, imprinting factors, and selectivity coefficients of BPA and its analogues.

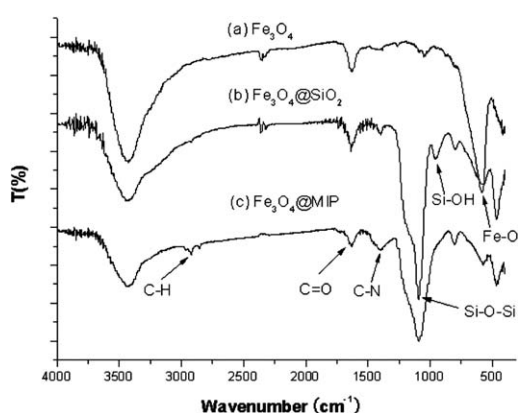


Fig. 3 FT-IR spectra for Fe₃O₄, Fe₃O₄@SiO₂, and Fe₃O₄@MIP.

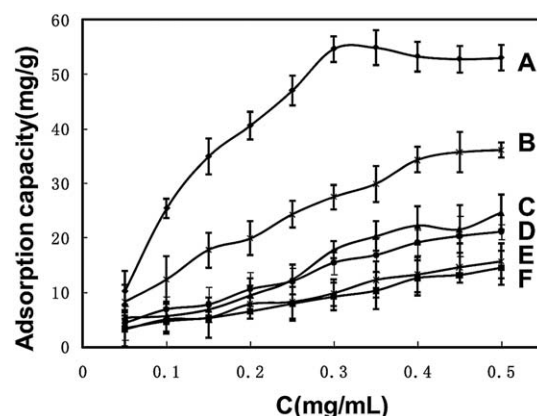


Fig. 4 Amount of bisphenol A bound by (A) Fe₃O₄@MIP and (D) Fe₃O₄@NIP; amount of bound BDAGE by (B) Fe₃O₄@MIP and (E) Fe₃O₄@NIP; amount of bound 4-OP by (C) Fe₃O₄@MIP and (F) Fe₃O₄@NIP.

The distribution coefficients, K , of the selected BPA between the polymeric particles and the solution was calculated by use of the formula:

$$K = C_p/C_s$$

where C_p is the amount of target molecules bound by the Fe₃O₄@MIP and C_s is the concentration of target molecules remaining in solution. Additionally, the imprinting factor (IF) and selectivity coefficient (α) were generally used to evaluate the selectivity properties of the imprinted and control NP toward BPA and the structurally related compounds BADGE and 4-OP. IF and α were calculated by use of the formulae:

$$\text{Imprinting factor } IF = K_i/K_c$$

$$\text{Selectivity coefficient } \alpha = IF_{BPA}/IF_i$$

where K_i and K_c represent the distribution coefficients of the analyte for the imprinted and control NP. IF_{BPA} and IF_i are the imprinting factors for BPA and its analogues.

Table 1 showed that the distribution coefficient, imprinting factor, and selectivity coefficient for BPA were much higher than for its analogues BADGE and 4-OP. The imprinting factor of BPA was almost two and four times higher than that of BADGE and 4-OP, respectively. These results verified that Fe₃O₄@MIP was highly specifically for BPA.

Table 1 The distribution coefficients, imprinting factors, and selectivity coefficients of BPA and its analogues for the imprinted and control NP^a

Target	K_{MIP}	K_{NIP}	IF	α
BPA	213.74 ± 3.69	38.78 ± 0.41	5.51 ± 0.43	—
BADGE	78.24 ± 1.35	29.21 ± 0.33	2.68 ± 0.065	2.06 ± 0.011
4-OP	37.77 ± 0.65	26.63 ± 0.47	1.42 ± 0.043	3.89 ± 0.008

^a In this experiment, 50 mg imprinted and control NP were incubated in a mixed solution of BPA, BADGE, and 4-OP at concentrations of 0.1 mg mL⁻¹ for 10 min at 25 °C ($n = 3$).

Optimization of extraction conditions

Effect of solution pH. Solution pH plays an important role in the adsorption of target compounds by affecting the existing form of target compounds and MIP. In this study, we placed MIPs at a amount of 25 mg in contact with a standard solution containing the analytes at 100 ng mL⁻¹ in a buffer at pH 3.2–11.0 for 30 min. As shown in Fig. 5A, a large drop in the recovery was observed at a pH value of 3.2 or 11.0. At low pH, some of the

MIPs could be degraded, and at high pH, the polarity of the target molecule and hydrophobic interactions could be increased, which reduces the enrichment efficiency. The state of BPA in the sample was influenced by the pH. Under weakly alkaline conditions, most of the BPA was in a molecular state, enhancing adsorption by the $\text{Fe}_3\text{O}_4@\text{MIP}$ sorbent. Hydrogen bonding could also contribute to the molecular recognition. The adsorption ability was highest near pH 8.9. Thereby, pH 8.9 was selected for subsequent experiments.

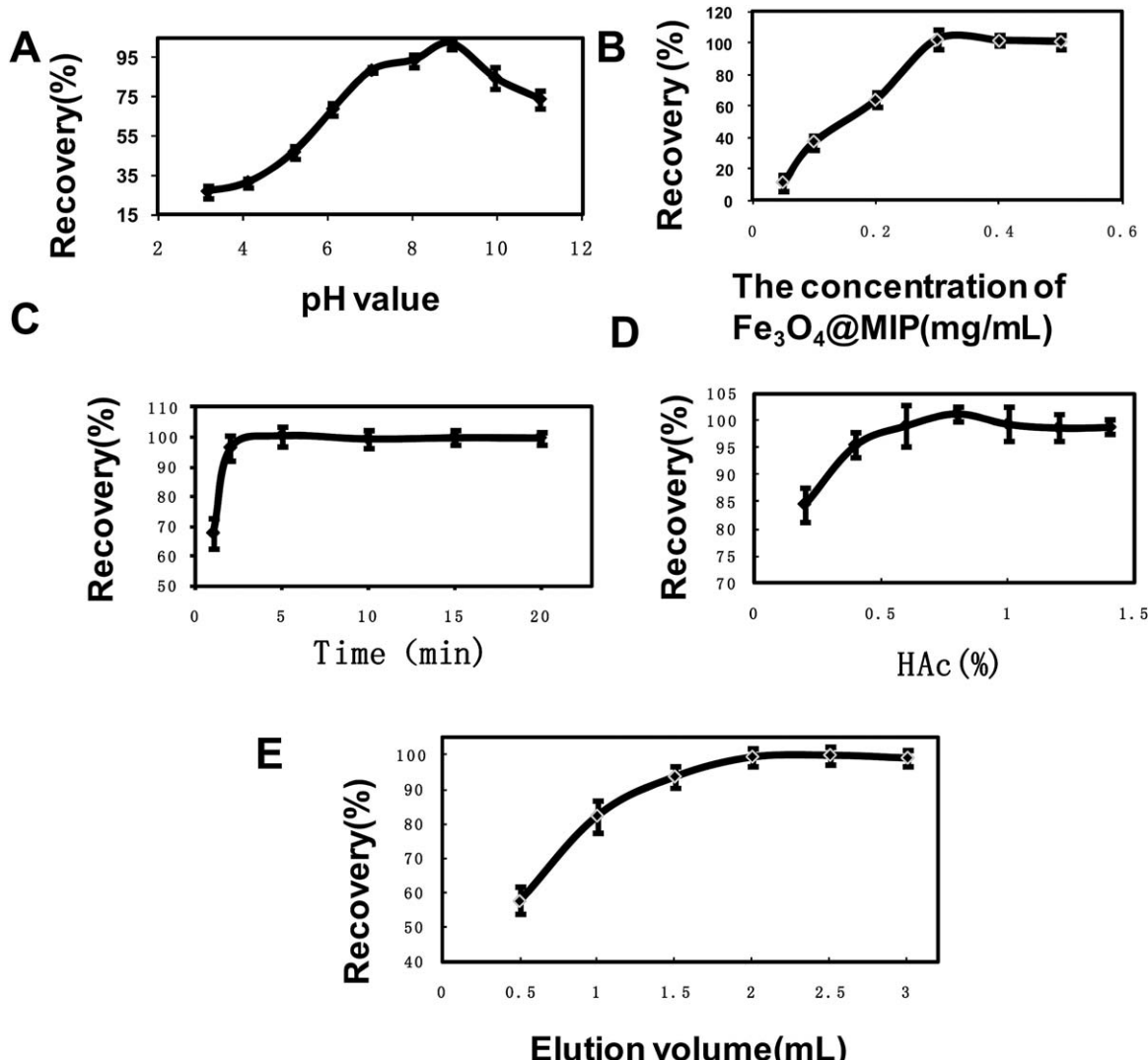


Fig. 5 Effects of (A) the pH of the sample, (B) the mass of sorbent, (C) the adsorption time, (D) the amount of HAc in the eluent and (E) elution volume on the extraction efficiency. Tests were carried out with 50 mL of a purified water sample spiked with 100 ng mL⁻¹ BPA.

Table 2 Analytical parameters of the proposed method for determining BPA in canned orange and milk samples, as well as LODs of the methods reported in previous studies

Sample	Linear range (ng mL ⁻¹)	Linearity (R^2)	LOD ^a (ng mL ⁻¹)	RSD ^b (%)	RSD ^c (%)	LODs obtained in previous works ^d (ng mL ⁻¹)
Canned orange	0.5–100	0.9987	0.1	6.4	10.5	4.5, ³⁷ 2.0 (Honey), ³⁸ less than 1.0 (Wine) ³⁹
Milk	1–100	0.9965	0.3	8.9	12.6	0.7, ⁴⁰ 0.2 ⁴¹

^a LOD for the present method, based on the signal being three times as large as the baseline noise (S/N = 3). ^b Intraday and $n = 5$. ^c Interday and $n = 5$.

^d LODs of methods reported in the references listed in the column.

Effect of amount of $\text{Fe}_3\text{O}_4@\text{MIP}$ sorbents. During the extraction procedure, the $\text{Fe}_3\text{O}_4@\text{MIP}$ sorbent was dispersed in the water to rebind analytes. The minimum amount of sorbent required for efficient recovery was then investigated. Amounts of $\text{Fe}_3\text{O}_4@\text{MIP}$ sorbent ranging from 0.05 to 0.5 mg mL⁻¹ were applied to 100 mL samples. It was found that 0.3 mg mL⁻¹ of sorbent enabled almost complete recovery of BPA, and increasing the amount of sorbent beyond this level could not produce any improvement in the recovery (Fig. 5B). Therefore, the amount of sorbent used was fixed at 0.3 mg mL⁻¹. After each extraction, the sorbent was easily recovered by rinsing with methanol. The recycling of the sorbent was then studied, and the results showed that the sorbent can be used at least 5 times with the same extraction efficiency.

Effect of extraction time. The extraction procedure includes three steps: adsorption, isolation, and desorption. The total time required for extraction is a key factor in the efficiency of the assay. As described for the MSPE procedure, the interaction between BPA and the sorbent is promoted by agitation. The effect of adsorption time was studied by varying the stirring time (0–20 min). Fig. 5C indicates that 3 min is sufficient to achieve a complete recovery. After the adsorption stage, the $\text{Fe}_3\text{O}_4@\text{MIP}$ in suspension can be isolated in 1 min using an external magnet. The adsorption time of $\text{Fe}_3\text{O}_4@\text{MIP}$ is shorter than that of ATRP-MIP³³ and other magnetic-MIP,²³ which may arise

since thin MIP layers of $\text{Fe}_3\text{O}_4@\text{MIP}$ have the potential to overcome mass transfer limitations. The whole extraction procedure can be accomplished within 5 min, which is superior to conventional SPE,² solid-phase microextraction,³⁴ and stir bar adsorptive extraction.³⁵

Effect of desorption solvent and volume. It is believed that the MIPs ability to adsorb analytes may be primarily due to the dramatic hydrogen bonds between BPA and pyridyl. A small amount of acetic acid allows the disruption of hydrogen bonding without any major impact on the polymer morphology.³⁶ In this study, an elution solvent of methanol containing acetic acid (0–1.4%, v/v) was evaluated. As can be seen from Fig. 5D, the recovery barely changed as the proportion of acetic acid was increased further, from 0.6% to 1.4%. Therefore, 0.6% acetic acid was used in subsequent experiments.

Theoretically, the greater the volume of eluent, the more completely the analytes are eluted from the adsorbent. In the view of economy and environmental protection, it is necessary to optimize the elution volume. As shown in Fig. 5E, when the methanol volume ranged from 0.5 to 2 mL, the recovery of analytes increased dramatically and reached a maximum when the volume was above 2 mL. So, it was concluded that 2 mL eluent was enough to remove the analytes from the adsorbent.

Analysis of milk and canned orange samples. HPLC-FLD provided an efficient tool for sensitive and selective

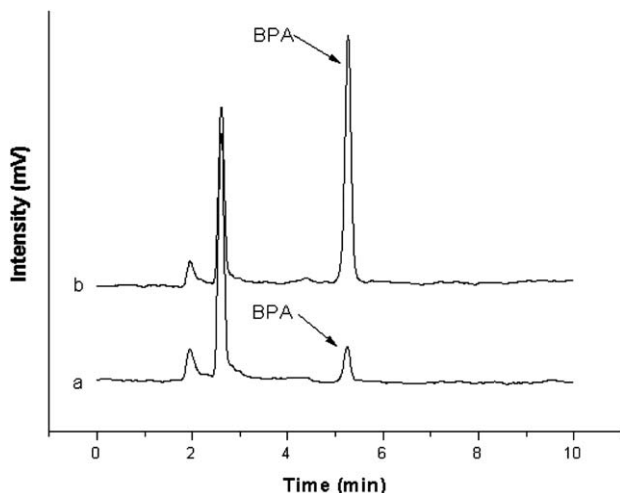


Fig. 6 MSPE/FLD chromatograms for (a) a real canned orange sample (BPA 1.27 ng mL⁻¹) and (b) a spiked canned orange sample (BPA 20 ng mL⁻¹).

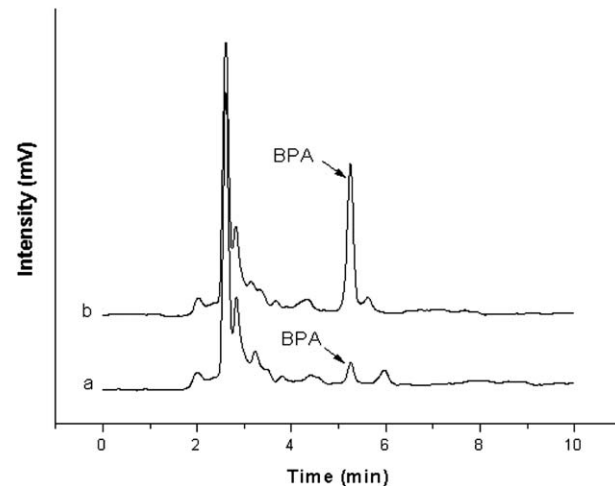


Fig. 7 MSPE/FLD chromatograms for (a) a real milk sample (BPA 0.81 ng mL⁻¹) and (b) a spiked milk sample (BPA 20 ng mL⁻¹).

determination of BPA from canned orange and milk samples. Matrix effects, including pH, protein precipitation and dilution, were eliminated before performing the MSPE procedure. The pH in canned orange was changed by buffer. The protein in milk was precipitated by zinc acetate and potassium ferrocyanide, and the precipitated protein was rinsed with methanol to avoid the adsorption of BPA onto it. The supernatant and the eluate were pooled and further diluted to reduce matrix effects. BPA was analyzed under the above-optimized conditions. Under the HPLC conditions described in section 2, BPA was eluted at 5.2 min in a clear peak. The chromatograms confirmed that BPA in spiked canned orange or milk were enriched by the $\text{Fe}_3\text{O}_4@\text{MIP}$ and can be recovered by washing. Therefore, the applicability of $\text{Fe}_3\text{O}_4@\text{MIP}$ for the extraction of BPA from canned orange and milk has been demonstrated.

To evaluate the accuracy and application of the developed method, milk and canned orange spiked with BPA were analyzed. At each concentration, five measurements were performed (Table 2). The calibration curves for canned orange and milk ranged from 0.5 to 100 ng mL⁻¹ and from 1 to 100 ng mL⁻¹, with R^2 values of 0.9987 and 0.9965, respectively. Recovery tests were performed at three spiked levels (5, 20, and 100 ng mL⁻¹) to evaluate the accuracy of the method. The recoveries of BPA from canned orange and milk were in the range of 83–107% and 72–113%, respectively. The relative standard deviations (RSD) were less than 13% for all the targets tested, and the LODs were less than 0.3 ng mL⁻¹ (estimated relative to the density of milk, S/N = 3). It could be seen that the proposed method has a lower LOD than most of the SPE-LC-MS methods,^{38,40} and the method involving LLE-HPLC-FLD³⁷ (Table 2).

The BPA contents of five canned orange and pure milk samples purchased from a market were determined using the present method. Chromatograms of the real and spiked canned orange and milk samples are shown in Fig. 6 and Fig. 7. BPA was found in these samples at levels of 0.41–1.34 ng mL⁻¹. The canned orange and milk were probably contaminated by the plastic packaging and the paint of the can wall, respectively, or the BPA may have found its way into the packed food in a variety of ways. The levels of BPA found in this study are much lower than the European Union migration limits of 3 mg kg⁻¹ for food.³

Conclusion

In this research, superparamagnetic $\text{Fe}_3\text{O}_4@\text{MIP}$ sorbents were successfully synthesized and applied for the enrichment of BPA from large volumes of packed food samples. Compared with traditional SPE methods, this SPE method has the following merits: (a) superparamagnetic $\text{Fe}_3\text{O}_4@\text{MIP}$ sorbents can be dispersed directly in packed food samples to extract analytes, then collected and eluted with the aid of a magnet, which avoids time-consuming packing of the SPE column and filtration operation. (b) The $\text{Fe}_3\text{O}_4@\text{MIP}$ can adapt to the complex food matrix, which owes much to the SiO_2 and MIP shell. (c) The $\text{Fe}_3\text{O}_4@\text{MIP}$ sorbents combine the advantages of nanoparticles and MIPs. The large surface area of nanomaterials and good selectivity of MIPs result in high adsorption capacity and specific extraction for target compounds, therefore, satisfactory results are achieved using a lower amount of $\text{Fe}_3\text{O}_4@\text{MIP}$ sorbents than common sorbents. This research has been applied to determine

the BPA contents of canned orange and milk samples. The proposed method could thus be a promising alternative for assaying complex food samples.

Acknowledgements

This work is financially supported by the National Natural Science Foundation of China (21071066, 20835006, 91027038), the 11th Five Years Key Programs for Science and Technology Development of China (2008BAK41B03, 2009BAK61B04, 2008ZX08012-001, 2010GB2C100167), and grants from Natural Science Foundation of Jiangsu Province, MOF and MOE (BK2010001, BK2010141, 2010DFB3047, JUSR11019, 201110060, 201110016, 201110061, 201010078, 201010216, 200910013, 200910083, 200910011, 200910277).

References

- 1 C. Erler and J. Novak, *J. Pediatric Nursing*, 2010, **25**, 400–407.
- 2 A. Schechter, N. Malik, D. Haffner, S. Smith, T. R. Harris, O. Paepke and L. Birnbaum, *Environ. Sci. Technol.*, 2010, **44**, 9425–9430.
- 3 L. Grumetto, D. Montesano, S. Seccia, S. Albrizio and F. Barbato, *J. Agric. Food Chem.*, 2008, **56**, 10633–10637.
- 4 J. Sajiki, F. Miyamoto, H. Fukata, C. Mori, J. Yonekubo and K. Hayakawa, *Food Addit. Contam., Part A*, 2007, **24**, 103–112.
- 5 M. Imanaka, K. Sasaki, S. Nemoto, E. Ueda, E. Murakami, D. Miyata and Y. Tonogai, *J. Food Hyg. Soc. Jpn.*, 2001, **42**, 71–78.
- 6 F. X. Perrin, T. Minh Hanh Nguyen, T. My Linh Tran and J. L. Vernet, *Polym. Test.*, 2006, **25**, 912–922.
- 7 B. Shao, H. Han, D. Li, Y. Ma, X. Tu and Y. Wu, *Food Chem.*, 2007, **105**, 1236–1241.
- 8 Q. Gao, D. Luo, J. Ding and Y.-Q. Feng, *J. Chromatogr., A*, 2010, **1217**, 5602–5609.
- 9 Q. Li, M. H. W. Lam, R. S. S. Wu and B. Jiang, *J. Chromatogr., A*, 2010, **1217**, 1219–1226.
- 10 L. Sun, L. Chen, X. Sun, X. Du, Y. Yue, D. He, H. Xu, Q. Zeng, H. Wang and L. Ding, *Chemosphere*, 2009, **77**, 1306–1312.
- 11 Q. Zhang, F. Yang, F. Tang, K. Zeng, K. Wu, Q. Cai and S. Yao, *Analyst*, 2010, **135**, 2426–2433.
- 12 X. Zhao, Y. Shi, T. Wang, Y. Cai and G. Jiang, *J. Chromatogr., A*, 2008, **1188**, 140–147.
- 13 L. Zhu, D. Pan, L. Ding, F. Tang, Q. Zhang, Q. Liu and S. Yao, *Talanta*, 2010, **80**, 1873–1880.
- 14 Y. Deng, D. Qi, C. Deng, X. Zhang and D. Zhao, *J. Am. Chem. Soc.*, 2007, **130**, 28–29.
- 15 S. Zhang, H. Niu, Z. Hu, Y. Cai and Y. Shi, *J. Chromatogr., A*, 2010, **1217**, 4757–4764.
- 16 Y. Li, T. Leng, H. Lin, C. Deng, X. Xu, N. Yao, P. Yang and X. Zhang, *J. Proteome Res.*, 2007, **6**, 4498–4510.
- 17 Y. Li, X. Xu, D. Qi, C. Deng, P. Yang and X. Zhang, *J. Proteome Res.*, 2008, **7**, 2526–2538.
- 18 Y. Li, Y. Liu, J. Tang, H. Lin, N. Yao, X. Shen, C. Deng, P. Yang and X. Zhang, *J. Chromatogr., A*, 2007, **1172**, 57–71.
- 19 Chen, W.-Y. Chen, P.-J. Tsai, K.-Y. Chien, J.-S. Yu and Y.-C. Chen, *J. Proteome Res.*, 2006, **6**, 316–325.
- 20 T. Jing, H. Du, Q. Dai, H. Xia, J. Niu, Q. Hao, S. Mei and Y. Zhou, *Biosens. Bioelectron.*, 2010, **26**, 301–306.
- 21 K. Takeda, A. Kuwahara, K. Ohmori and T. Takeuchi, *J. Am. Chem. Soc.*, 2009, **131**, 8833–8838.
- 22 K. Yang, M. M. Berg, C. Zhao and L. Ye, *Macromolecules*, 2009, **42**, 8739–8746.
- 23 Y. S. Ji, J. J. Yin, Z. G. Xu, C. D. Zhao, H. Y. Huang, H. X. Zhang and C. M. Wang, *Anal. Bioanal. Chem.*, 2009, **395**, 1125–1133.
- 24 L. Qin, X.-W. He, W. Zhang, W.-Y. Li and Y.-K. Zhang, *J. Chromatogr., A*, 2009, **1216**, 807–814.
- 25 X. Wei, X. Li and S. M. Husson, *Biomacromolecules*, 2005, **6**, 1113–1121.
- 26 X. Li and S. M. Husson, *Biosens. Bioelectron.*, 2006, **22**, 336–348.
- 27 H. Kong, C. Gao and D. Yan, *J. Am. Chem. Soc.*, 2003, **126**, 412–413.
- 28 K. Matyjaszewski, T. E. Patten and J. Xia, *J. Am. Chem. Soc.*, 1997, **119**, 674–680.

29 Q.-Q. Gai, F. Qu, Z.-J. Liu, R.-J. Dai and Y.-K. Zhang, *J. Chromatogr., A*, 2010, **1217**, 5035–5042.

30 C.-H. Lu, W.-H. Zhou, B. Han, H.-H. Yang, X. Chen and X.-R. Wang, *Anal. Chem.*, 2007, **79**, 5457–5461.

31 C.-H. Lu, Y. Wang, Y. Li, H.-H. Yang, X. Chen and X.-R. Wang, *J. Mater. Chem.*, 2009, **19**, 1077–1079.

32 Y. Li, W.-H. Zhou, H.-H. Yang and X.-R. Wang, *Talanta*, 2009, **79**, 141–145.

33 G. Q. Wang, Y. Q. Wang, L. X. Chen and J. Choo, *Biosens. Bioelectron.*, 2010, **25**, 1859–1868.

34 F. Tan, H. Zhao, X. Li, X. Quan, J. Chen, X. Xiang and X. Zhang, *J. Chromatogr., A*, 2009, **1216**, 5647–5654.

35 F. Canale, C. Cordero, C. Baggiani, P. Baravalle, C. Giovannoli and C. Bicchi, *J. Sep. Sci.*, 2010, **33**, 1644–1651.

36 G. Karasová, J. Lehotay, J. Sádecká, I. Skačáni and M. Lachová, *J. Sep. Sci.*, 2005, **28**, 2468–2476.

37 C. Sun, L. P. Leong, P. J. Barlow, S. H. Chan and B. C. Bloodworth, *J. Chromatogr., A*, 2006, **1129**, 145–148.

38 E. Herrero-Hernandez, R. Carabias-Martinez and E. Rodriguez-Gonzalo, *Anal. Chim. Acta*, 2009, **650**, 195–201.

39 C. Baggiani, P. Baravalle, C. Giovannoli, L. Anfossi and G. Giraudi, *Anal. Bioanal. Chem.*, 2010, **397**, 815–822.

40 N. C. Maragou, E. N. Lampi, N. S. Thomaidis and M. A. Koupparis, *J. Chromatogr., A*, 2006, **1129**, 165–173.

41 D. K. Alexiadou, N. C. Maragou, N. S. Thomaidis, G. A. Theodoridis and M. A. Koupparis, *J. Sep. Sci.*, 2008, **31**, 2272–2282.